Paving the path between low- and high-mass star formation : dynamics probed by Herschel far-infrared spectroscopy

San Jose Garcia, I.

1 Introduction

1.1. Star formation process

"Stars form in molecular clouds". Behind this apparently simple and widely used sentence lies a whole field of astrophysics that is still maturing. To fully understand the star formation process, we must begin with the nurseries of stars, which are called Giant Molecular Clouds (GMCs).

GMCs are large (10-100 pc), relatively dense ($\sim 10^2$ cm^{-3}) and cold ($\sim$10 K) regions of the interstellar medium (ISM) (e.g. Bergin & Tafalla 2007) with a filamentary structure. The origin of this complicated network of filaments is related to supersonic turbulence in the ISM, which pushes and compresses low-density gas into layers (Myers 2009; André et al. 2014). This filamentary complex does not necessary create one single connected structure and only groups of filaments, called bundles, may have a common physical origin (Hacar et al. 2013). Those groups of velocity-coherent filaments that reach high enough densities to become gravitationally unstable will start contracting, becoming denser and eventually fragmenting into self-gravitating cores in hydrostatic equilibrium (see André et al. 2010). Therefore, the formation of a core is dominated by turbulence and gravity. This also means that not all GMCs will meet the right conditions to host the formation of a new generation of stars. Those clouds containing filaments which do no reach densities above the critical value will not fragment into cores, as, for example, in the Polaris molecular cloud (more details in André et al. 2010).

Gravitationally bound cores are located radially along the filaments and will grow while the filamentary structures contract from the inside-out and while there is still available surrounding gas (Myers 2013; Kirk et al. 2013; Henshaw et al. 2014). Large bundles of filaments and those which overlap and merge are the precursors of massive cores (Myers 2009; Schneider et al. 2012) while low-mass cores come from the gas of a single piece of filament. From this point on, once the precursor core of a future star is created, the evolution of these young stellar objects (YSOs) is tightly related to their initial mass and the specific environmental conditions which will shape their growth. This work aims to reveal if the paths that describe the evolution of low- (M<2 $M_\odot$), intermediate- (2≤M<8 $M_\odot$) and high-mass (M≥8 $M_\odot$) YSOs interlace, diverge or overlap.

1.1.1. Low-mass young stellar objects

Evolution and phases

The dense, small, and gravitationally-bound cores resulting from filament fragmentation will form low-mass stars, and are called *prestellar cores*. Due to the absence of a source of internal energy, these cores cool and contract reaching high densities and become gravitationally unstable. The strong gravitational pull on the surroundings draws more material in and gives rise to the collapse of individual cores.

In the centre of these collapsing cores a new object is formed: a *protostar*. This is deeply embedded in a thick envelope, and accretes material from the collapsing large-scale core through an accretion disk (Terebey et al. 1984). The protostellar phase then begins in which the luminosity of the central object is mostly derived from accretion process. Due to the rotation of the system and the conservation of angular momentum, this disk gradually flattens even if the infall of the surrounding material is isotropic. Moreover, the rotation and accretion of the central object together with the presence of magnetic fields triggers the formation of bipolar jets perpendicular to the disk, which remove part of the excess angular momentum accumulated during the accretion process.

These jets inject energy and momentum into the surrounding envelope, and dig cavities in it. Between the cavities and the envelope gas, an intermediate layer is created, called the outflow cavity wall. In this region, envelope material is entrained and exposed to winds and ultraviolet (UV) radiation from the forming star. The complex interplay between these structures (cavity, outflow cavity wall, jet, stellar wind) dictates the evolution of a protostar and the removal of surrounding cloud material. Their ensemble constitutes the molecular outflows (see simplified sketch in Fig. 1.1), and together with the protostar, envelope and disk form a *young stellar object* (YSO).

Up to this point, a YSO is considered to be in its earliest, most embedded phase: Stage 0 (André et al. 1993; Robitaille et al. 2006, 2007). The mass of the collapsing envelope is significantly larger

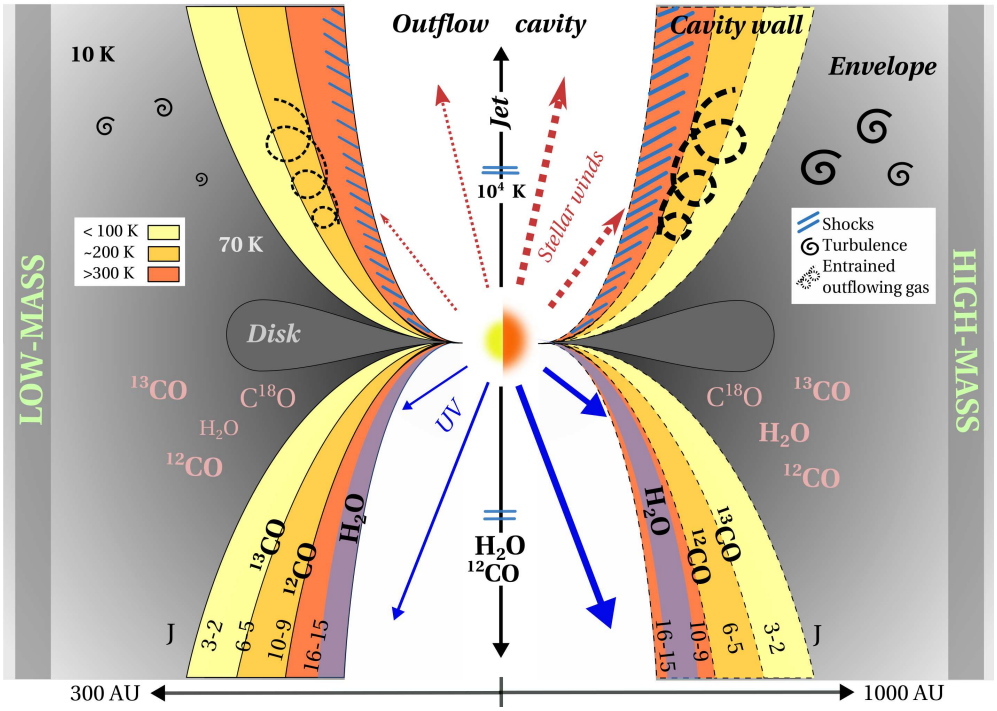

Figure 1.1: Cartoon illustrating the different components within the outflow, together with the temperature distribution and the location of the water and CO isotopologue emission in a low-mass (*left*-side) and high-mass (*right*-side) YSO. Turbulent motions are indicated with spirals, the entrained outflowing material with swirls and shocks with small blue lines. The UV radiation and stellar winds are indicated with blue and dotted red arrows respectively, which are thicker in the *right*-side of the figure to highlight that radiation and winds are more energetic for high-mass YSOs than for their low-mass counterparts. The disk also generates winds but those have not been added to the figure for simplification. The typical scale for a low- and high-mass YSO is indicated by the horizontal black arrow at the bottom of the figure.

than that of the central object, so these protostars are still deeply embedded in a dusty environment and are thus usually not detectable in the near-infrared. The bulk of the emission from these objects is instead at sub-millimetre/far-infrared wavelengths. In Stage 0 objects, the bipolar outflows are particularly collimated and energetic due to the intense accretion rate of material onto the central protostar and the dense ambient gas.

During the evolution of the protostar, the disk grows and flattens, as a consequence of infall from the envelope and the angular momentum conservation, while the surrounding envelope gradually disperses due to two opposite mechanisms: the continued accretion onto the central star-disk system and the dissipation caused by the action of the powerful outflows. The protostar is then in Stage I, in which the protostellar mass becomes larger than the envelope mass. In this phase a YSO is less opaque and UV radiation from the central forming star penetrates further into the envelope, heating the disk as well. Therefore, objects in the Stage I start to be effectively observable at mid- and near-infrared wavelengths unless the source is observed edge-on. The outflow cavity also widens due to the dissipation of the ambient gas.

The star formation process then continues and the YSO reaches Stage II, which marks the beginning of the pre-main sequence phase because the luminosity of the central object is now dominated by its photosphere rather than by accretion. Stage II is characterised by the total removal of the envelope material and the presence of a prominent circumstellar disk surrounding now a pre-main sequence star. The mass of the disk is larger than that of the envelope and larger grains start to grow inside the disk, becoming the building blocks for the formation of planetary systems once

Table 1.1: Observational selection criteria for the more embedded phases of low-, intermediate- and high-mass YSOs.

Category	Type	Observational characteristic	Refs.
LM	Class 0	$L_{\rm bol}/L_{\rm submm} > 200$; $T_{\rm bol} < 70$ K	1, 2
	Class I	$L_{\rm bol}/L_{\rm submm} < 200$; 70 $< T_{\rm bol} < 650$ K; $\alpha^a > 0.3$	1, 2, 3
IM	Class 0/Type I	$T_{\rm bol} < 70$ K; $-2 < p_{1.3{\rm mm}}{}^b \leq -1$	2, 4
	Class I/Type II	70 $< T_{\rm bol} < 650$ K; $-1 < p_{1.3{\rm mm}}{}^b \leq 0$	2, 4
HM	HMPO IR-bright	Weak radio continuum; > 100 Jy at 12 μm	5
	HMPO IR-quiet	Weak radio continuum; Weak at mid-IR (< 100 Jy at 12 μm)	5
	Hot core	Emission from complex organic molecules (COMs)	6

Notes. LM: low-mass protostars (M<2 $M_\odot$); IM: intermediate-mass YSOs (2≤M<8 $M_\odot$); HM: high-mass YSOs (M≥8 $M_\odot$).
(1) André et al. (1993). (2) Myers & Ladd (1993). (3) Lada & Wilking (1984); Greene et al. (1994). (4) Fuente et al. (1998, 2002). (5) van der Tak et al. (2000); López-Sepulcre et al. (2010). (6) Cesaroni (2005).
$^{(a)}$ Spectral index, α, is a proxy of the slope of the SED between 2 and 20 μm. $^{(b)}$ The spatial index, p, measures the variation of the column density with the distance from the forming star. The values of this parameter depend on the mass tracer. Here we present those derived from 1.3 mm continuum observations, $p_{1.3{\rm mm}}$.

the accretion and outflows are completely gone (Stage III). From this point, $\sim 10^7$ years after the collapse of the pre-stellar core, the central object starts burning hydrogen and reaches the main-sequence, becoming finally a low-mass *star*.

Observational classification

The mentioned Stages (0–III), which mark the evolution of a low-mass protostar, are defined based on how the mass of the different physical structures within the YSO (envelope, central protostar, disk) vary and compare with time. However, since estimating these masses is difficult, originally the classification was based on the observed characteristics of YSOs at each evolutionary stage, the so-called *evolutionary classes*. Therefore, the concept of Classes was created before that of Stages. The different Classes derived observationally follow the evolution of low-mass YSOs and attempt to identify their evolutionary stage.

As mentioned before, the bulk of the emission of a YSO, quantified by its spectral energy distribution (SED), moves to shorter wavelengths as the object evolves (Lada & Kylafis 1999; André et al. 2000). The shape of the SED also changes with the different evolutionary stages of a low-mass YSO. Therefore, several methods have been developed to characterise the shape of the SEDs in order to link observational classes with evolutionary stages (Evans et al. 2009). Some of these methods are the calculation of the spectral index, α, which measures the slope of an SED between 2 and 20 μm (Lada & Wilking 1984; Greene et al. 1994). Since they are heavily extincted, this slope cannot be obtained for the Stage 0 protostars. In addition, the ratio between the luminosity at 350 μm and the bolometric luminosity, $L_{\rm bol}/L_{\rm submm}$, provides information about the relative mass of the central object with respect to its envelope (André et al. 1993). Another useful parameter is the bolometric temperature, $T_{\rm bol}$, which is the temperature of a blackbody with the same mean frequency as that of the object's SED (Myers & Ladd 1993). Table 1.1 indicates the interval of values of these observational parameters which define the two protostellar phases of a low-mass YSO, i.e., Class 0 and Class I.

When using these methods it is important to realise that the shape of a protostar SED may be affected by the inclination of the outflow-disk system with respect to the line of sight. Therefore, the study of the source geometry is required to correct for this bias and Stages and Classes do not uniquely correlate (van Kempen et al. 2009b).

The observational characteristics and parameters used to classify intermediate- and high-mass YSOs into the different Classes of their embedded phases are also summarised in Table 1.1 (see below for discussion).

Observational advantages and challenges of low-mass YSOs

The low-mass star formation process is better understood and more widely studied than that of its more massive counterpart for several reasons. First, many examples of low-mass YSOs can be studied within few hundreds of parsecs (pc), so the different physical components of a single protostar (disk, envelope, outflow, etc.) start to be spatially resolved with the current observational facilities. Second, low-mass stars represent 70–90% of the total stellar population. In addition, the lifetimes of low-mass YSOs are relatively long with a protostellar duration (Stages 0 and I) of ∼0.5 Myr (Dunham et al. 2014), so it is possible to study targets in the different evolutionary stages. Therefore, the sample of low-mass protostars is large enough to enable a solid statistical analysis of their properties, and improve our understanding of their formation and evolution.

However, these objects present some challenging aspects that need to be considered. Even though a significant fraction of stars forms in clustered environments (e.g. Bressert et al. 2012), traditionally the observed low-mass protostars are in relatively isolated conditions. One of the reasons is that their observations are easier to interpret due to the lack of contamination from neighbouring sources. As a consequence, the low-mass star formation scenario described in Sect. 1.1.1 is founded on what has been learned from isolated targets, and may not represent how most of such stars form. To account for the effect of surrounding sources on the formation and evolution of protostars, it is important to complete the catalogs with low-mass YSOs in clustered environments (see Bressert et al. 2010 for cluster definition), creating a representative sample. From the observational point of view, the acquisition of high quality data for low-mass YSOs is a more arduous task, because these objects are faint and a single source may subtend up to an arc-minute on the sky due to their proximity. Therefore, longer exposure times are required to obtain data with the same quality level of their massive counterparts and maps are needed to encompass the entire protostellar system.

1.1.2. High-mass young stellar objects

Theories

There are several scenarios proposed to explain the formation of high-mass stars (M_*≥8 $M_\odot$) which are still under debate since each of those addresses different observational aspects. Two of the three generally-recognised theories are based on the accretion of material from the parent cloud, while a third model advocates for merging or coalescence of pre-formed systems.

The first scenario involving accretion mechanisms is that of *monolithic collapse* presented by McKee & Tan (2003), which is considered a scaled-up version of the low-mass process. Once the filaments compress and fragment into starless cores (M∼100 $M_\odot$) or starless clumps (M∼1000 $M_\odot$), the over-densities of molecular gas condense creating a central protostellar object with bipolar outflows and an accretion disk. During this process, the dense YSOs try to maintain the equilibrium between gravity and turbulence in order not to fragment. This requires injecting mechanical energy into these systems, which is thought to happen through two mechanisms: either with outflows and accretion shocks or by bringing turbulence from the outside of the core in a cascade down to smaller scales sizes, creating an isotropic pressure. The warm photo-sphere of the protostellar object produces energetic UV radiation which creates a strong radiation pressure and threatens to dissipate the ambient material and stop the accretion (Kahn 1974). This can be overcome if the accretion rates are few orders of magnitude faster than in the low-mass counterparts (10^{-4}–10^{-3} $M_\odot$ yr^{-1} versus 10^{-7}–10^{-5} $M_\odot$ yr^{-1} respectively). When this happens, the radiation pressure shifts to the direction perpendicular to the disk (the so-called flash-light effect) and powers the outflows (Krumholz & Thompson 2007; Kuiper et al. 2015). As for low-mass star formation, the accretion happens locally in this scenario, so the mass that will end-up in the star is gathered before the process begins and a single massive star, or a multiply gravitationally bound system, forms from a single massive protostellar core. Therefore, this hypothesis for high-mass star formation follows the same prescriptions as for their low-mass counterparts, but with larger values of turbulence and accretion in order to overcome the radiation pressure and stop the core from fragmentation.

The second scenario is that of *competitive accretion* by Bonnell et al. (1997, 2001), where the parent cloud is gravitationally bound rather than supported by turbulence. In this model, the cloud fragments into protostars which will move relative to the molecular gas. So, contrary to the previous scenario, the actual material constituting the future star comes from several parts of the cloud, and is accreted while the formation process is already ongoing. This implies that, except for a circumstellar disk and envelope, no other material is associated with the object prior to its formation, and the compression phase is short-lived and transitional between the fragmentation and collapse of the cloud. The size of the accretion domain (i.e., the region from which the gas can be gathered) depends on the mass of the YSO, as a direct consequence of its gravity, and on its location within the cloud. This latter aspect refers to the fact that most of the gas within the cloud settles on the regions in the deepest parts of the gravitational potential. The YSOs forming close to those denser areas will have more gas available to add to their accretion domain and the highest chances of becoming more massive (and therefore expand their domains). Since the gas reservoir is limited within the cloud due to its finite mass, the protostars compete for the cloud mass and the accretion domains among neighbouring sources may overlap. The foundation of this model is the observational fact that massive stars form in clustered environments (Zinnecker & Yorke 2007) and that only a small number of starless massive cores have been observed.

Finally, the model based on the *stellar mergers* (Bonnell et al. 1998; Bonnell & Bate 2002) was born to explain the formation of the most massive stars (M>30 $M_{\odot}$), which are also the least common. In this scenario, star formation occurs on cluster scales with the fragmentation of the cloud into many low-mass protostars. The accretion of material by these objects dissipates the turbulent component from the cluster, which starts contracting. This process moves the protostars closer together, increasing the stellar density of the region, especially in the centre of the cluster. With stellar densities of the order of 10^7 stars pc^{-3}, collisions between low-mass protostars become a realistic possibility, due to the decrease of the impact parameters, and these objects may merge forming rapidly rotating massive stars. This scenario implies longer formation timescales, because low-mass protostars need to be formed first, and involves violent phenomena since the stellar collision would cause the destruction of any outflow or disk, and even the ejection of stars from the system.

Independently of the process, in general the formation time of a high-mass star is observationally constrained to be of the order of a few times 10^5 yr, which constitute a few % of their total life-time (Churchwell 2002; Mottram et al. 2011).

Observational classification

The lack of agreement on how high-mass YSOs form goes together with a poorly defined evolutionary trail. However, as for the low-mass protostars, certain observational aspects and features recognised in the object emission have been traditionally used to distinguish high-mass YSOs into different phases (see Table 1.1 for some examples, Churchwell 1999; van der Tak et al. 2000; Beuther et al. 2007; Zinnecker & Yorke 2007). Even if the following classification is purely observationally based, a rough evolutionary trail can be extracted from it. However, the evolution within the embedded stages cannot be unambiguously distinguished partly because these intermediate phases can coexist together and are subject to observational biases (e.g., van Dishoeck & van der Tak 2000).

We start with the massive analogues of prestellar cores: *high-mass starless cores*. These are dense ($\sim$$10^5$ cm^{-3}) and cold (10–20 K) cores formed after the fragmentation of the cloud, with typical sizes of 0.3 pc (Beuther et al. 2002; Williams et al. 2004; Garay et al. 2004). Their lifetimes may be short, of the order 10^4–10^5 yrs, as suggested by their low numbers (Tackenberg et al. 2012). Although Infrared Dark Clouds (IRDCs), whose name derives from the fact that they show absorption against the bright mid-infrared galactic background (Simon et al. 2006), may fulfil the previous description, they are rather considered molecular clumps or filaments. In addition, IRDCs are not always associated with the formation of high-mass stars and conversely, many of them already show ongoing star formation, so they cannot be considered truly starless systems.

High-mass protostellar objects (HMPOs) can be considered a protostar or embedded pre-main

sequence star whose central source is still not burning hydrogen. While outflows, masers and infall signatures are seen in these objects, no or only very weak ionising radiation is detected. In addition, these objects present a massive envelope with a gradient of temperature and density towards the centre. Within this phase, two sub-types are distinguished: mid-infrared-bright and mid-infrared-quiet HMPOs, which correspond to those objects with and without bright emission in the mid-infrared (at 12 μm in particular, see van der Tak et al. 2000; Motte et al. 2007; López-Sepulcre et al. 2010). This may reflect a difference in evolutionary stage but could also be due to geometry.

When sub-millimetre emission from Complex Organic Molecules (COMs) such as $HCOOCH_3$, CH_3OH, etc. is present, then the massive YSO is considered a *hot molecular core* (Cesaroni 2005). These complex molecules are formed because the central forming star warms an increasingly large area around it as it gains mass. As a consequence, ice mantles are evaporated from grains, adding complexity to the chemical composition of the surrounding gas and triggering gas-phase reactions. COMs may be present already in the HMPO phase, but the emission from these molecules may be weak or not observable. This can be because of the dense and opaque circumstellar envelope in which these massive protostars are embedded or because of beam-dilution of the small hot-core region in single-dish observations (van Dishoeck & van der Tak 2000).

Eventually, the stellar atmosphere of the central object produces enough UV radiation to ionise the surrounding material forming an *hypercompact* HII *region* (HCHII) or *ultracompact* HII *region* (UCHII) (see Kurtz 2005; Hoare et al. 2007, and references therein). The former is generally smaller and denser than the latter and may be still confined by the remnants of the infalling material and disk (Tan & McKee 2003; Keto 2007). To complicate the picture, HMPOs and hot cores can contain hyper- or ultracompact HII regions.

If the ionisation caused by the central star keeps expanding, reaching pc scales, and disrupting the parent cloud, then the YSO is considered a *compact* HII *region* and *classical* HII *region*. In the latter phase the ionisation is global and the massive star can be observed in the optical and near-infrared regime.

Observational advantages and challenges of high-mass YSOs

The difficulties in acquiring a clear understanding of the formation of high-mass objects are related to several observational challenges and the intrinsic properties of these rare objects. Although high-mass YSOs are bright, requiring relatively short observational exposure times, they are located at large distances (few kpc away) and are embedded in massive and clustered environments with hundreds of surrounding protostars. Therefore, the different components of these objects (outflows, disk, envelope), as well as their physical conditions, are difficult to resolve spatially with the available telescopes and observational techniques. In addition, their envelopes are opaque during their entire formation. Finally, the emission from massive YSOs may be contaminated by the neighbouring objects, which adds another layer of complexity to interpret these observations from the physical and chemical point of view.

The high-mass star population is smaller than that constituted by their low-mass counterparts, which means that by default there are fewer massive YSO candidates available for study. In addition, once the accretion has stopped, they evolve rapidly, reaching the main-sequence (Churchwell 2002). This is the reason why it is hard to derive an evolutionary sequence for high-mass YSOs.

1.2. From low- to high-mass

Having put in context both low- and high-mass star formation, it is inevitable to lay out the hypothesis that high-mass YSOs may be scaled-up versions of their low-mass counterparts. The work presented in this thesis aims at achieving a more comprehensive understanding of the star formation process across the mass range by investigating in which conditions that hypothesis holds. As a first step, we present the main similarities and differences between low- and high-mass YSOs from the theoretical and observational point of view to build the ground for their comparison and

study. Intermediate-mass YSOs are introduced as a potential bridge between these two sub-groups of objects.

Similarities

Studies have shown that high-mass YSOs present collimated molecular outflows (Beuther et al. 2002; Shepherd 2005) and disks (Cesaroni et al. 2007) as low-mass protostars do, particularly up to 10^4 $L_\odot$ (see Fig. 1.1). These observations seem to support the turbulent core accretion model (McKee & Tan 2003), analogous to the low-mass star formation process but involving a larger turbulent regime, higher accretion rates and stronger stellar winds (McKee & Ostriker 2007a). Even if the major cause of the outflows and their driving agent may change with the mass of the YSO (see next section), the dynamical properties of their shocked and entrained material do not seem to be affected by the mass of the central forming star. In addition, the higher mass infall rates observed in their envelopes are consistent with the higher mass accretion rates required to form high-mass stars within $\sim 10^5$ yr.

High-mass YSOs form in denser environments and show larger fractions of companion objects than their low-mass counterparts, consistent with the scaled-up hypothesis. In addition, studies performed decades ago already presented correlations between the bolometric luminosity of the sources, considered as a proxy of their mass, and several physical parameters such as their bipolar mass outflow rate (Shepherd & Churchwell 1996), and their circumstellar envelope mass (Chandler & Richer 2000). This correlation extends over a large range of $L_{\rm bol}$ (from 0.3 to 10^5 $L_\odot$). Norberg & Maeder (2000), Behrend & Maeder (2001a) and Shepherd (2003) present a possible link between the accretion and outflow rates that does not depend on the mass of the central forming star. This relation suggests the presence of common mechanisms regulating the flows of both entrained and accreting material in these systems.

Differences

The prime difference between low- and high-mass YSOs lies in the definition of a protostar itself. A protostar is a gaseous system in hydrostatic equilibrium which is still not burning hydrogen and derives most of its luminosity from accretion. While low-mass objects spend all their evolution period in the embedded phase as true protostars, high-mass YSOs reach the main-sequence from their very beginnings, burning hydrogen during most of the formation process (Yorke & Bodenheimer 2008). In addition, the main-sequence temperature of the central object's photosphere and disks increases with stellar mass, which moves the peak of the stellar blackbody into the UV regime. This means that massive YSOs generate stronger UV radiation than their low-mass analogues. However, these distinctions are not a mere matter of definition, and they are not limited to the duration of protostellar, pre-main sequence and main-sequence phases (Blum 2005) or the peak frequency of the stellar emission. They influence other crucial aspects as well. To start with, while the luminosity of a low-mass protostar is dominated by the radiation generated by shocks during the accretion process, the luminosity of high-mass YSOs comes mostly from their warm photosphere. According to the protostellar and pre-main sequence phase definition for the low-mass objects, high-mass YSOs should then be considered pre-main or main-sequence stars (depending if they are already burning hydrogen or not). Furthermore, the energetic UV radiation in these latter objects, both coming from their stellar atmospheres and inner disks, ionises the surrounding gas creating an intense radiation pressure which could stop the accretion of material onto the forming star, as previous explained. It causes as well the photo-evaporation of the accretion disk and the protostellar envelope of the massive object and neighbouring lower-mass systems. These radiative forces play a significant role in the formation of massive YSOs but their effects are negligible for low-mass protostars. Another difference is related to the lifetimes of these objects, which are shorter because their contraction period is shorter than that of low-mass protostars (and comparable to the accretion time). In addition, high-mass YSOs also emit non-ionising radiation which causes the dissociation of molecules such as H_2 and CO. For this to happen, radiation above 11.0 eV needs to be generated, a range not accessible by low- and intermediate-mass YSOs.

The physical origin and the driving agent of molecular outflows is still under debate (Arce et al. 2007; Frank et al. 2014). For low-mass protostars, outflows are created as a consequence of the extra angular momentum dissipation in the form of bipolar jets and magneto-centrifugal forces of the stellar winds, mechanisms that keep powering this structure. On the other hand, for high-mass YSOs, the removal of angular momentum (jets) may be backed up by powerful stellar winds and strong radiation pressure (flash-light effect) as cause and driving mechanism of molecular outflows.

As for the theories explaining the star formation, the competitive accretion and stellar mergers scenarios acquire significance in clustered environments, more common among massive YSOs and for which a larger amount of protocluster gas needs to be accreted. These theories cannot be applied to the formation of low-mass objects in isolation and diverge from the scaled-up hypothesis. In addition, the clustering allows dynamical interactions between the forming YSOs (increasing the kinetic energy of the system) that may cause the ejection of objects (runaway OB stars, e.g. de Wit et al. 2005). This process does not seem to happen in regions that only form distributed, low-mass stars.

Finally, high-mass YSOs have a more significant effect on the environment than their less massive counterparts. Expanding HII regions could compress gas from neighbouring clumps and trigger a new generation of star formation or actually blow-out the gas of nearby systems destroying their change of becoming stellar nurseries.

Intermediate-mass YSOs as the bridge between low- and high-mass

Between 2 and 8 $M_{\odot}$ stands a sub-group of YSOs that shares specific properties from both their less and more massive counterparts, describing the transition between these two mass regimes (see review by Beltrán 2015). Far from making them an appealing type of YSOs for study, not many systematic observations towards them have been done since the interpretation of their emission becomes challenging given that these objects are at larger distances than their low-mass counterparts and fainter than massive YSOs. Therefore, their formation and evolutionary stages are uncertain.

Despite the small statistics, these YSOs are found both in isolated and clustered environments (Hillenbrand et al. 1995; Kumar et al. 2006), constituting the bridge towards the denser clusters in which high-mass objects form (Testi et al. 1999). The fragmentation of their parent cloud does not seem to depend on the luminosity of the core (Palau et al. 2013), and some intermediate-mass regions have a single luminous source (e.g., van Kempen et al. 2012; Palau et al. 2013) while others are composed of a collection of lower-mass YSOs (Beltrán et al. 2002, 2008; Neri et al. 2007; van Kempen et al. 2012).

In general, previous studies suggest that the formation mechanism of an intermediate-mass YSOs is a scaled-up version of that of their less massive counterparts. A protostellar phase may be possible to be defined for the intermediate-mass objects, but the analogous low-mass Class 0 and Class I phases are difficult to distinguish because their earliest stages remain deeply embedded within the dusty cloud (Nielbock et al. 2003). In addition, the structure of these objects seems to resemble that of a low-mass protostar since molecular outflows and circumstellar disks have been observed and detected for a handful of objects (see Takahashi et al. 2008; Beltrán et al. 2008; Sánchez-Monge et al. 2010; van Kempen et al. 2012, for some examples). Intermediate-mass sources are characterised with more massive and energetic outflows and larger accretion rates than those measured for low-mass protostars. However, the intrinsic complexity of these YSOs is similar to that of low-mass protostars and early-B type objects (Calvet et al. 2004; Fuente et al. 2001). Finally, the photosphere of intermediate-mass YSOs reaches high enough temperatures to emit UV radiation and trigger complex chemistry processes which lead to the formation of COMs (Fuente et al. 2005; Sánchez-Monge et al. 2010).

To summarise, there is still a lot of work to be done in order to characterise this peculiar and interesting group of YSOs. The study of these objects can shed some light onto the global understanding of the star formation process by marking the transition between several physical and chemical conditions present in these objects and in low- or high-mass YSOs (or in both).

Why does it matter?

Contraction times, radiation flows, formation theories, gravitational dynamics: it might look like these basic differences between low- and high-mass YSOs are more significant than their similarities, which would dispel the scaled-up hypothesis. However, the intrinsic complexity of each single object, the large and varied range of physical and chemical processes taking place across all these systems, and the observational biases discourage the hunt for any possible resemblance among YSOs. For this reason, any trend or common characteristic discerned across a varied sample of objects is worth a deeper investigation, because it may point to some fundamental physical properties of the star formation process, important enough to stand out over the inherent differences of each YSO. Examples and evidences are the presence of both outflows and disks in low-, intermediate- and high-mass YSOs (Beuther et al. 2002; Zhang et al. 2001; Cesaroni et al. 2007; Boley et al. 2012) and the similar dynamical conditions which seem to govern the shocked gas along the outflow cavity wall independently of the object mass (chapter 4). Therefore, the study of the star formation as a function of luminosity on scales of individual protostars could benefit the global understanding of this process for example, by identifying which specific physical and dynamical processes are not affected by the mass of the central forming star. This study could also help to discriminate among the different high-mass star formation theories and interpret observational biases due to source distances and telescope's limitations.

1.3. Methodology

1.3.1. Molecules as diagnostics

The spectrum of an object reveals information about its internal structure and properties (e.g., composition, temperature), in the same way that a piece of DNA does for a living creature. Molecular lines carry the information to interpret the physical and chemical conditions of YSO environments. Infrared and sub-millimetre spectroscopy are crucial techniques to dig inside these cold and embedded objects. Molecules emit or absorb radiation at specific frequencies, which are defined by the transition between two quantised energy levels. The distribution of the energy levels, also called energy diagram, is unique to each molecule, and the collection of possible transitions between energy levels constitutes its molecular fingerprint.

At infrared and sub-millimetre wavelengths two types of molecular transitions take place: *vibrational* and *rotational* transitions. The former are defined by oscillatory motions of atoms within the molecule which generate radiation at infrared wavelengths. The latter, designated with the quantum number J, are established by the rotation of the molecule around its axes. Rotational transitions are detected in emission in the far-infrared to millimetre regime only for gaseous species with a permanent dipole moment. Due to the relatively small spacing between rotational states, these transitions can be measured at high spectral resolution ($R = \lambda/\Delta\lambda \geq 10^6$), which allow us to resolve and interpret line profiles. While the frequency of a spectral line is influenced by the relative motion of the target and the observer, its broadening or more generally its shape depends on the motions intrinsic to the studied region within the YSO. Doppler-broadening is the dominant process that causes the broadening of these lines, since the motions of the gas particles with respect to the observer cause the emitted radiation to span a larger range of frequencies around its rest-frame value. Therefore, the specific physical properties of the gas being traced are reflected in the line shape of its molecular transitions, so that they generate distinct signatures.

Although detecting a transition already gives us information about the environmental conditions (e.g. presence of violent shocks, UV field regime, densities and temperatures present), it is the study of spectrally resolved line profiles that shed light on the velocity structure of the gas. This kinematic information can be extracted by decomposing the line profiles into different velocity components and by characterising their width, intensity and central frequency value. This procedure allows us to distinguish, for example, between quiescent gas, which moves at relatively low velocities with respect to the rest-frame, outflowing material, that reaches larger velocities (tens

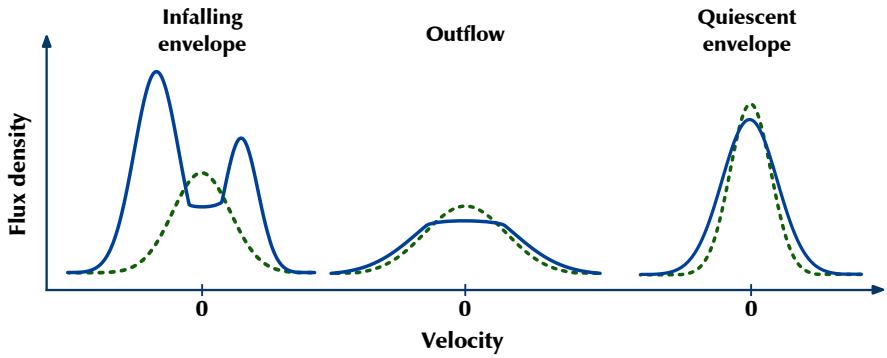

Figure 1.2: Comparison of the typical line profile signatures created by an optically thick (τ_ν >>1) and an optically thin (τ_ν <1) transition (solid and dashed line, respectively), which probe infall gas (*left*), material moving at large velocities in the outflow (*middle*) and quiescent gas from the envelope (*right*). Figure by M. Persson.

of km s^{-1}) and shocked gas along the jet, which appears largely offset from the source velocity (Bachiller et al. 1990; Kristensen et al. 2012; Mottram et al. 2014). In addition, if at a specific frequency the optical depth, τ_ν, of a molecular transition is larger than unity, (i.e., a photon at that frequency is more likely to be re-absorbed than to escape the system) then motions such as rotation, expansion and infall leave a characteristic and recognisable footprint in those molecular lines (see Fig. 1.2 for examples). However, in order to determine the origin and cause of rotational line emission, as well as its optical depth, it is crucial to know the intrinsic properties of the studied molecule and transitions: their critical densities ($n_{\rm cr}$), the molecules dipole moment, etc.. Some of the physical and chemical properties of protostellar systems such as excitation temperatures, densities and abundances can be derived by combining the spectroscopic analysis of several molecules and different rotational transitions.

Due to the importance of sub-millimetre spectroscopy to the study of star formation, in the last decades a lot of effort has been put into improving and expanding the available observatory facilities and in acquiring high quality data. All millimetre telescopes share similar technical principles and setups: a parabolic collecting area (or antenna), a receiver that amplifies the detected signal, and a spectrometer that processes this signal (a more detailed explanation of the observational process is given in Sect. 1.4). There are two types of millimetre telescopes: *interferometers*, composed of an array of antennas, and *single-dish*, with only one large parabolic collecting area, which deliver the data highlighting either the small or large spatial scales. Interferometers provide information on small spatial scales, necessary to resolve disks and disentangle the emission from distant and crowded systems. Single-dish telescopes cover larger spatial scales at high spectral resolution, crucial for achieving a more complete picture of large structures (outflows, envelope), and large-scale motions (infall or turbulence at envelope sizes). The spatial resolution of an interferometer is given by the distance between the antennas and that of a single-dish depends on the size of its parabolic collecting area. While interferometers filter out the emission from spatial scales larger than that given by the shortest distance between two antennas in the telescope array, the reduced angular resolution of single-dish telescopes smear the emission coming from small regions over the resolution element, complicating the interpretation of the data.

In this thesis we present single-dish velocity-resolved data. We mitigate the lack of spatial resolution by studying molecular tracers which are known to probe specific physical conditions in YSOs and structures of protostellar systems that may be smaller than the beam resolution. With this method we keep the large-scale view while information on smaller spatial scale regions is added indirectly. The molecular tracers selected to disentangle the dynamical conditions of envelope and outflows are ^{12}CO, ^{13}CO, C^{18}O and H_2O. Their characteristics and potential are further explained in the next section.

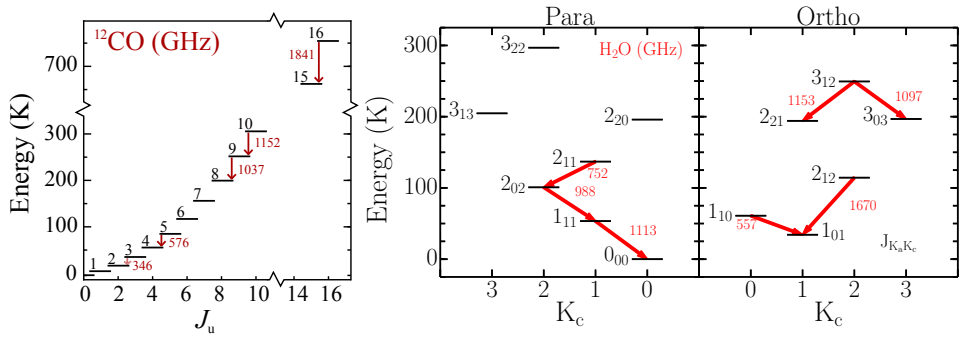

Figure 1.3: (*Left*) ^{12}CO energy diagram up to J=16. (Figure updated by M. Persson from U. A. Yıldız Phd thesis). (*Right*) Para- and ortho-water energy diagram. The ^{12}CO and H_2O transitions observed with *Herschel*-HIFI are indicated with red solid arrows while the ^{12}CO $J = 3$–2 transition, observed from ground-based telescopes, is marked with a red dashed line. The frequency of each of these rotational transitions is shown in GHz.

1.3.2. CO and H_2O as key molecular tracers

After H_2, the second most abundant molecule in our Universe is carbon monoxide, a pivotal molecule in many fields of astronomy. CO is present in all parts of protostellar systems: from the envelope, to the bipolar outflow and disk. It has been widely targeted by infrared and sub-millimetre observations of Galactic and extragalactic objects (Kennicutt & Evans 2012, and references therein).

CO has traditionally been observed not only because it can be detected throughout the YSO, but also because it is a reliable tracer of the dynamical and excitation properties of the these environments as a result of its intrinsic properties. CO has a small permanent dipole moment ($\sim$ 0.1 Debye). At far-infrared and sub-millimetre wavelengths, the critical densities of the rotational transitions are relatively low, so CO is easily excited by collisions with H_2, even in low density regions. In these conditions, the CO gas can be safely considered to be in local thermal equilibrium (LTE), which simplifies the interpretation of the rotational lines because the excitation temperature, $T_{\rm ex}$, is then equal to the kinetic temperature of the gas, $T_{\rm kin}$. Thus, the measure of different CO rotational transitions provides an excellent estimate of the gas kinetic temperature of the system.

The most abundant CO isotopologue (therefore producing the strongest lines) is $^{12}C^{16}O$ (^{12}CO). To probe the cold gas, both in the envelope and outflow, low-rotational ^{12}CO transitions ($J\leq3$) are used, with upper energy levels, $E_{\rm up}$, between 10–50 K. This means that, since a pure-CO ice layer deposited on a grain evaporates at $T_{\rm eva}\simeq$20 K (Collings et al. 2004; Öberg et al. 2005; Bisschop et al. 2006), the bulk of the observable CO at sub-millimetre wavelengths is in the gas phase, except maybe in the coldest gas ($T_{\rm kin}<$20 K). However, the inner regions of the envelope closer to the actual forming star are hidden by these outer colder layers, as well as most of the entrained and shocked material across the outflow are warmer (50–300 K), so rotational transitions with higher $E_{\rm up}$ are required. The emission of mid-J ^{12}CO lines ($4\leq J\leq10$) around the targeted frequency probes warmer, quiescent envelope material. On the other hand, the entrained outflowing material, which moves at larger velocities with respect to the rest-frame of the observer, is traced by the blue- and red-shifted emission with respect to the source velocity (Snell et al. 1980). This weaker emission covering a large range of frequencies is generally identified as the line-wings of the detected emission line including the higher-J ones (e.g., Curtis et al. 2010; Yıldız et al. 2012, 2013). Finally, even warmer regions are then traced by higher-J ($J>10$) lines (van Kempen et al. 2010; Green et al. 2013; Karska et al. 2013; Manoj et al. 2013) and violent processes, such as shocks along the outflow or jet, are probed by the line wings of ^{12}CO transitions (Kristensen et al. 2013). The different values of the upper energy levels and the frequency of selected low-, mid and high-J ^{12}CO rotational transitions are given in the left energy diagram of Fig. 1.3.

The rotational emission lines of the CO isotopologues ^{13}CO and $C^{18}O$ are also detected in pro-

tostellar systems. These isotopologues show similar energy level diagrams at sub-millimetre wavelengths to ^{12}CO with comparable intrinsic molecular properties. Given the characteristic isotopic ratios, ^{13}CO and C^{18}O are less abundant and the emission lines are usually weaker and narrower than those measured for ^{12}CO. Since its lines are optically thin and not contaminated by outflow emission, C^{18}O is a good tracer of quiescent envelope material, especially the high-J transitions which probe inner warmer areas. ^{13}CO emission probes the dense envelope material as well, but part of the emission is associated with gas located at the edges of the outflow walls which is heated by UV radiation from the forming star (Spaans et al. 1995; van Kempen et al. 2009a; Yıldız et al. 2012). In addition, by assuming a CO/H_2 abundance ratio, an estimate of the molecular gas mass of the system can be made. To conclude, the study of the ^{12}CO, ^{13}CO and C^{18}O rotational lines provides an important and detailed picture of the protostellar structure, its dynamics, temperature and gas distribution and outflow activity.

From the chemical and observational point of view, H_2O is a more challenging molecule than CO. Water is one of the dominant compounds of oxygen and the most abundant species in ice mantles (van Dishoeck et al. 2013). Due to its high binding energy, H_2O freezes out on the grains at temperatures below 100 K. This means that water is present in the outer colder part of protostellar envelopes mainly in the solid phase and mostly in warm regions of YSO environments in its gaseous form. For this reason, its rotational lines not only probe the warm gas but they also reflect the significant abundance variations between regions of the YSO at different temperatures.

Water has a larger dipole moment (1.85 Debye) and Einstein A coefficients than CO, so the critical densities are also larger. This means that H_2O shows intense line emission even when sub-thermally excited. Since the two hydrogen spins can be oriented either perpendicular or parallel, this molecule comes in two forms: para- and ortho-H_2O. The right panel of Fig. 1.3 shows the H_2O energy diagrams of the para and ortho ladders together with the frequencies of selected transitions. Water molecules are generally formed through three routes in the gas phase: at high- and at low-temperatures, and on the grains (e.g. Ioppolo et al. 2008, 2010; Cuppen et al. 2010; van Dishoeck et al. 2013; Lamberts et al. 2014). However, since a considerable water reservoir is in the ice mantles, violent processes involving high velocity material, such as shocks, can also add H_2O into the gas phase through sputtering from the grain (Codella et al. 2010; Van Loo et al. 2013; Neufeld et al. 2014; Suutarinen et al. 2014). Therefore, significant water abundances are likely to be measured in the outflows, in particular in the outflow cavity or along the jets where the stellar winds or the material ejected in the outflow system encounters the entraining gas and powerful shocks take place (see Fig. 1.1). Because in these types of dramatic processes the gas reaches high temperatures and velocities, this gas can potentially be traced by the emission of the line-wings of H_2O rotational transitions (Kristensen et al. 2010, 2012, 2013; Nisini et al. 2010; Mottram et al. 2014; Santangelo et al. 2014).

In summary, due to its properties, water is a robust tracer of the warm gas, the energetic processes present in the star formation regions, such as shocks along the outflows, and the dynamical structures of these environments.

1.3.3. Analysis tools

In the case of Local Thermal Equilibrium (LTE), i.e., when the excitation of molecules is dominated by collisions, the kinetic temperature of the gas can be approximated to the measured excitation temperature $T_{\rm ex}$. The value of $T_{\rm ex}$, as well as other parameters such as the column density, $N_{\rm tot}$, can be derived from the line profiles of several rotational transitions. However, when the LTE conditions cannot be assumed because the system is sub-thermally excited (its density is lower than a critical value $n_{\rm cr}$ and the de-excitation is dominated by radiation rather than collisions) and the level populations cannot be characterised by a single excitation temperature, then the non-LTE approach has to be taken (see review by van der Tak 2011).

Since the information about chemical abundances, temperature and density distribution, velocity structure and dominant motions (turbulence, expansion, infall) is coded into the observed line profiles, we need radiative transfer tools to model and compare them to the data, so that these parameters can be constrained.

In general, any radiative-transfer code solves the radiative transfer equation (Eq. 1.1), which describes how an emitted photon, at a specific frequency, interacts with the particles met along a straight path in the line of sight.

$$\frac{dI_\nu}{dz} = -\kappa_\nu I_\nu + j_\nu, \tag{1.1}$$

The observed intensity, I_ν, is the result of the balance between absorption and emission (which fractions are given by the κ_ν and j_ν coefficients, respectively), after integrating along the line of sight travelled by the radiation, whose coordinates are defined by z. The sources of absorption and emission are microscopic processes causing the excitation and de-excitation of the particles along that path. These processes are spontaneous emission, stimulated emission, absorption of radiation as well as particle collision which can excite or de-excite the gas particles. The probability of these processes are determined by the Einstein A and B coefficients and the collisional rate coefficient C, values which are unique to each molecular transition and collisional partner.

The radiative transfer equation across a system in non-LTE can be solved by including those observed molecular transitions for which the above coefficients are available. Usually the problem needs to be simplified with a series of assumptions, as we will mention below. Depending on which parameters need to be constrained, on the structure of the medium, and on the geometry of the problem, several radiative transfer codes have been developed.

For systems that can be considered isothermal and homogeneous, the single kinetic temperature and column density value characterising the medium can be constrained using one-dimensional non-LTE radiative transfer codes such as RADEX[1] (van der Tak et al. 2007). Different geometries of the emitted system can be assumed as well, from static spherical to plane-parallel (also called "slab"). As output, this code provides the line intensities, optical depth and excitation temperatures of the studied molecular transitions. These are then compared to those calculated from the observations. An example of the power of combining observations and these radiative transfer codes is given in chapter 4, where the excitation conditions of the post-shocked material along the cavity outflow are estimated from the analysis of the excited water lines and assuming a slab geometry of the water emitting area.

When the distribution of temperature, density and velocity cannot be assumed to be uniform across the system, or the kinematical structure needs to be derived, or the effects of turbulence, infall, expansion, and rotation on the emission lines need to be determined, more complex codes solving the radiative transfer and excitation of molecular lines are required. In this thesis we use the spherically symmetric non-LTE radiative transfer code RATRAN (Hogerheijde & van der Tak 2000) to constrain the dynamics of protostellar envelopes using rotational lines of optically thin and thick tracers (chapter 3). The spherical envelope under study is subdivided in cells, and for each cell it is possible to define the specific temperature, density (as explained in the next paragraph) and velocity structure. This code also generates synthetic line profiles that are compared to the profiles of the observed transitions. In addition, the level populations and optical depth of these transitions are also provided. The potential of this code is based on the freedom to define the physical structure of a system with spherical or axial symmetry, and on the possibility of constraining the dominant motions causing the broadening of the observed line profiles.

The density of a protostellar envelope, n, varies with distance, r, from the central forming star as a power-law with index p ($n \propto r^{-p}$). This index is determined for each YSO from the fitting of the far-infrared SED combined with the spatial extent at 450 and 850 μm. Those are the wavelengths at which the dust re-emits most of the absorber stellar radiation. Therefore, the luminosity of the central star and the properties of the dust (opacity, size, etc.) define the dust temperature. Continuum radiative transfer codes are used to derive the temperature and density distribution of a protostellar envelope by assuming a power-law density distribution with a given p index. In those codes, the gas and dust temperature are considered equal and further parameters, such as envelope size and dust opacities, need to be defined. DUSTY (Ivezić & Elitzur 1997) or HOCHUNK3D (Whitney et al. 2013; Robitaille 2011, hereafter WR) are widely used codes to constrain the temperature and density profiles of low- and high-mass YSOs respectively. In particular, DUSTY models the

[1] http://home.strw.leidenuniv.nl/~moldata/radex.html

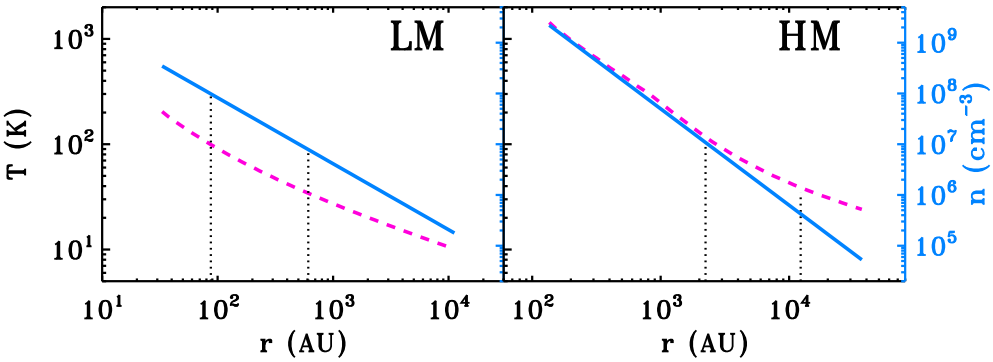

Figure 1.4: Temperature (T, pink dashed line) and density profiles (n, blue solid line) of a low-mass (LM; *left*) and a high-mass (HM; *right*) YSO as a function of the radius of the modelled envelope (distance from the central star). The vertical black dotted lines indicate the radii at which the gas and dust temperature reaches 100 and 35 K respectively.

observed SED sub-millimetre and spatial distribution of an object by modifying the previously mentioned parameters and using the opacity values calculated by Ossenkopf & Henning (1994) (further information of the procedure in Kristensen et al. 2012). Examples of the density and temperature profile for a low- and a high-mass YSO are shown in Fig. 1.4 (for more details read chapter 3).

1.4. *Herschel* Space Observatory - HIFI

High-J CO lines cannot be observed from the ground due to atmospheric absorption at sub-millimetre wavelengths, so the warmer inner regions of protostellar systems are not observable with this species. In addition, water cannot be observed in Galactic sources except in a few weak $H_2^{18}O$ lines, which prevents us from achieving a more comprehensive picture of the dynamical structure of YSO environments, especially across the outflows. However, in May 2009 the *Herschel* Space Observatory (Pilbratt et al. 2010), an ESA cornerstone mission, was launched which aimed to explore the molecular Universe at far-infrared and sub-millimetre wavelengths at significantly greater sensitivity and resolution than any previous space telescope (e.g. *ISO*, *SWAS*, *ODIN*, *IRAS*). Its scientific objectives were focused on studying dusty and relatively cool objects; particularly the birth of stars and their interaction with the interstellar medium, and the formation and evolution of galaxies in the early Universe.

Herschel was equipped with a 3.5 m diameter primary mirror and three instruments: a very high resolution spectrometer, the Heterodyne Instrument for the Far Infrared (HIFI; de Graauw et al. 2010); an imaging photometer and integral field line spectrometer, the Photodetector Array Camera and Spectrometer (PACS; Poglitsch et al. 2010); and an imaging photometer/Fourier transform spectrometer, the Spectral and Photometric Imaging Receiver (SPIRE; Griffin et al. 2010). The operational lifetime of the *Herschel* Space Observatory finally concluded on June 17, 2013.

This thesis primarily focuses on the analysis of HIFI observations, therefore a more detailed description of this instrument is given. This single-pixel heterodyne spectrometer was designed to provide very high spectral resolution, between 0.3 and 0.03 km s^{-1} (1.1 and 0.125 MHz), over a frequency range of approximately 480–1250 GHz and 1410–1910 GHz (625–240 and 213–157 μm). The diffraction limit at a frequency of 548.8 GHz was 42″, reaching 21″ at a frequency of 1101 GHz. This angular resolution was a factor of 3–5 higher than that achieved by previous sub-millimetre space missions such as *SWAS* or *Odin*.

At sub-millimetre wavelengths there are no good amplifiers available to amplify the detected weak emission. However, HIFI combines the heterodyne technique with superconducting detector

technology to be able to convert the detected signal to lower frequencies, for which amplifiers are available, while preserving the initial spectral information. The instrument worked by mixing the incoming signal, f_s, with another very stable and monochromatic signal, generated by a local oscillator, f_{LO}. The output is a much lower frequency signal called intermediate frequency (IF = $| f_s - f_{LO} |$), which is easier to amplify at radio wavelengths and is then sent to the spectrometer for spectral analysis. Therefore, the specific IF frequencies could be generated by two different source signals: $f_s > f_{LO}$ or $f_s < f_{LO}$. Considering this for a range of incoming frequencies, each channel of the spectrometer was sensitive to two frequency values at the same time, so two superimposed portions of an object's spectrum were measured resulting in the *double sideband* (DSB) reception. The portion of the source spectrum above the f_{LO} is designated as upper sideband (USB) and that below f_{LO} as the lower sideband (LSB).

The mixing process was carried out in 7 heterodyne receiver bands with dual horizontal (H) and vertical (V) polarisations. They were divided into two groups according to the mixer device used and the instantaneous frequency covered. Bands 1 to 5 use Semiconductor-Insulator-Semiconductor (SIS) mixer technology, which operated at 480–1250 GHz with a bandwidth of 4 GHz. Bands 6 and 7 have Hot Electron Bolometer (HEB) mixers and those covered the 1410–1910 GHz frequency range with a bandwidth of 2.4 GHz.

HIFI had four spectrometers or backends, namely; a Wide Band Spectrometer (WBS) and a High Resolution Spectrometer (HRS) with two polarisations each, horizontal (H) and vertical (V). The WBS was an Acousto-Optical Spectrometer (AOS) which covered the full IF range available at a single resolution of 1.1 MHz. The HRS was an Auto-Correlator System (ACS) with several possible resolutions (from 0.125 to 1.00 MHz). The bandwidth of this latter backend could be split to sample more than one portion of the available IF range.

Finally, HIFI provided three *Astronomical Observing Templates* (AOTs): "single pointing" (AOT I); "mapping" (AOT II) and "spectral scanning" (AOT III). For each of them there were different observing modes namely dual-beam switch (DBS), position switch (PSw), frequency switch (FSw) and load chop.

The HIFI WBS single pointing observations presented in this thesis were taken in dual-beam switch mode. This means that for each source only one position on the sky was targeted at one specific frequency, and during the observation the beam was moved to two reference positions $3'$ either side of the source position using fast chopping.

Further details on the reduction and scientific interpretation of HIFI data are given in the Observation sections of chapters 2, 4 and 5. In addition to the HIFI observations, spectrally resolved ^{12}CO and C^{18}O $J = 3$–2 data from ground-based facilities such as the JCMT and APEX are included to extend the analysis of these YSOs to their colder, lower density regions, achieving a more comprehensive picture of these embedded systems.

1.4.1. WISH

Water is present not only in the coldest regions of protostellar environments constituting the ice mantles of grains, but also in gaseous form probing warmer material and energetic processes such as shocks along the outflows. For this reason, the guaranteed-time *Herschel* key programme "Water In Star-forming regions with *Herschel*" (WISH[2]; van Dishoeck et al. 2011) observed this molecule and other species such as CO with unprecedented spectral and angular resolution with the purpose of investigating the physical and chemical structure of a large and diverse sample of sources related to star formation. In particular, this programme follows water abundances, kinematics and excitation through the evolutionary sequence of ∼80 sources (from pre-stellar cores to gas-rich disks) and across a vast range of luminosities (L_{bol} from < 1 to $> 10^5$ $L_\odot$).

Single point observations and small maps of H_2O, its less-abundant isotopologues ($H_2^{17}O$ and $H_2^{18}O$) and chemically related species such as OH, H_2O^+ and H_3O^+ were targeted with HIFI and PACS around the protostar position and the outflows. The study of water in the initial embedded

[2] https://www.strw.leidenuniv.nl/WISH/

environments, crucial to understand not only the formation of protoplanetary systems but ultimately also the origin of life, is complemented with observations of high-frequency lines of ^{12}CO, ^{13}CO and C^{18}O. These molecules not only help to improve the dynamical knowledge of protostellar systems and the gas kinetic temperature, but also provide a reference frame to determine the abundance of species such as H_2O with respect to H_2 and ensure a self-consistent data set for analysis.

Complementing the WISH project, the water and CO HIFI data from two follow-up *Herschel* programmes are also included in chapter 5. The first one, the "William Herschel Line Legacy" survey (WILL; PI: E.F. van Dishoeck, Mottram et al., in prep.) observed water and CO for an unbiased sample of 45 low-mass protostars. The second, "Water emission from outflows and hot cores in the Cygnus X protostars" (PI: S. Bontemps), focused on observing three water transition across the 86 most luminous YSOs across the Cygnus X region. The aim of including these additional programs is to expand the study initiated by WISH and test the significance of the achieved results by improving the statistics of the analysis with a more uniform sample of YSOs filling the gaps left by WISH, especially from the observational point of view. Further details about these two surveys are given in chapter 5.

1.5. This thesis

This thesis presents velocity-resolved HIFI H_2O data and mid-J ($J \leq 10$) ^{12}CO, ^{13}CO and C^{18}O observations for 51 embedded YSOs drawn from the *Herschel* key programme WISH. In addition, low-J CO transitions from ground-based single-dish telescopes are included to compare the physical conditions of the inner and warmer regions of YSO environments to those of the outer colder parts. The sample of objects, composed of 26 low-mass protostars, six intermediate-mass sources and 19 high-mass YSOs, covers a large range of bolometric luminosities $L_{\rm bol}$ (from < 1 to $>10^5$ $L_\odot$), several evolutionary stages within the embedded phase and different physical scales (as compared in Fig. 1.4).

The purpose of this work is to investigate the physical and dynamical structure of protostellar environments across a wide luminosity range (as illustrated in Fig. 1.5) by characterising the H_2O and CO spectra in terms of line profile and line luminosity. The studied species are unambiguous tracers of specific physical conditions within the YSO. In addition, excitation and kinematical information of certain protostellar regions is extracted from the emission lines using the non-LTE radiative transfer codes RADEX and RATRAN. The ultimate goal is to broaden our understanding of the star formation process without imposing luminosity boundaries, and to put in context these processes on Galactic and extragalactic scales.

The main questions we address with this work are:

- Which type of information can be extracted from a basic analysis of the CO line profile and line luminosity? How do CO lines change as a function of luminosity and what does that tell us? Is there any trend, proxy of an underlying mechanism, measurable from low- to high-mass YSOs?
- Do motions such as infall and turbulence scale with the mass of the YSOs? What are the main non-thermal motions which cause the broadening of the C^{18}O lines? How different are the velocity and C^{18}O abundance structures from low- to high-mass?
- From which regions of the YSOs does the water emission originates across the studied sample of YSOs? What dynamical conditions in the outflow cavity walls can the excited water lines constrain? Are high-J (J>10) CO transitions tracing shocked gas as water does in low-, intermediate- and high-mass YSO environments? How are the water excitation conditions affected by the mass of the central forming star?
- Are the results obtained from the WISH programme biased by the sample selection or can they be extrapolated to more standard sources? What can we learn from large surveys and how do we link with extragalactic samples?

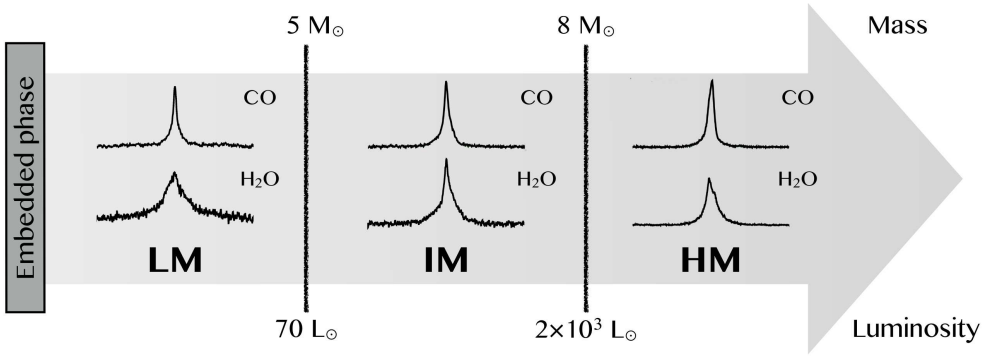

Figure 1.5: Averaged and normalised ^{12}CO $J = 10$–9 (*top*) and H_2O 2_{02}-1_{11} (*bottom*) spectra for the WISH low-mass Class 0 protostars (LM), intermediate-mass (IM) and high-mass YSOs (HM). All spectra are plotted on the same velocity range (from -100 to 100 km s^{-1}) to compare the observations of these two species across the entire mass and luminosity range studied with WISH. The arrow indicates the adopted mass and luminosity values that delimit each sub-group of YSOs. This figure illustrates the focus of this thesis: the study of the mass/luminosity trail with observations of CO and water.

These questions are addressed across the chapters of this thesis, which are summarised as follows:

Chapter 2 presents the ^{12}CO, ^{13}CO and C^{18}O velocity-resolved data for the WISH sample of YSOs (see San José-García et al. 2013). For low- and intermediate-mass objects the width of the C^{18}O line profiles increases at higher-J transitions, which indicates that either the level of turbulence is larger in the inner regions of the envelope or other non-thermal motions are at work broadening the profile (see chapter 3). For massive YSOs, this width does not vary with J. Finally, the distance-normalised line luminosity of the HIFI CO lines correlates with the source bolometric luminosity out to extragalactic scales. This suggests that, independently of the mass of the YSO, high-J CO transitions primarily trace the amount of dense gas associated with the system (see Fig 1.6).

Chapter 3 aims to quantify the contributions of turbulence and infall to the broadening of line profiles of optically thin low- and high-J C^{18}O transitions and optically thick HCO$^+$ lines for a sub-sample of low- and high-mass YSOs (San José-García et al. submitted). The non-LTE radiative transfer code RATRAN is used for this purpose. In order to reproduce the analysed line profiles, both infall and turbulent motions are required. The turbulent width increases with $L_{\rm bol}$, but for the infall motions this trend is only seen in sources with $L_{\rm bol} > 10^3$ $L_\odot$. In addition, for these high-mass YSOs, the best-fit infall component is slower than the maximum infall velocity estimated from their assumed stellar masses. Finally, the derived best-fit values of the turbulent velocities are slightly larger than those calculated for systems in virial equilibrium, which suggests that turbulence prevails over the gravitational potential once star formation is ongoing.

Chapter 4 shows the excited water transitions observed across the WISH sample of YSOs and compares the results to those mid-J ($J\leq10$) and high-J ($J>10$) ^{12}CO transitions (San José-García et al. submitted). More than 60% of the water emission originates from non-dissociative shocks in the outflow cavity wall. The remaining emission comes from dissociative shocks for low-mass Class 0 objects and from the quiescent envelope in the case of Class I protostars, intermediate- and high-mass YSOs. For low-mass protostars, only high-J ($J>10$) CO rotational transitions seem to probe similar kinematical properties to those traced by H_2O. In the case of massive YSOs, the gas traced by both the CO $J = 10$–9 and 16–15 lines is linked to that probed by the excited water lines, probably as a consequence of the injection of strong turbulence by the UV radiation of these massive objects (see bottom-right quadrants of Fig. 1.1). A correlation between the line luminosity and $L_{\rm bol}$ is also measured for these H_2O lines and extended to extragalactic scales.

Chapter 5 presents a similar study as discussed in chapter 4 but for a larger and unbiased

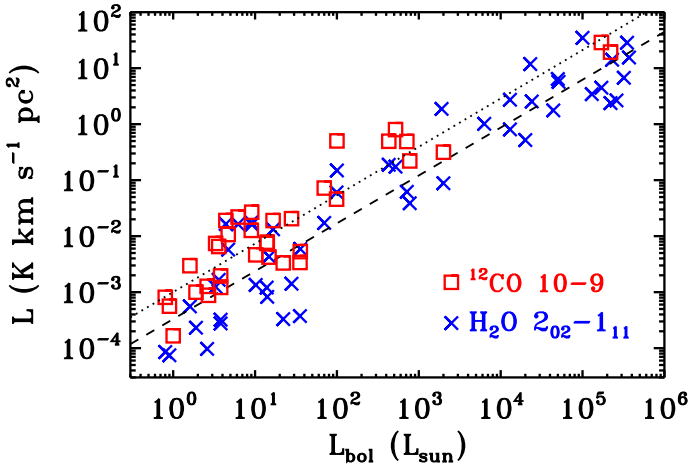

Figure 1.6: Line luminosity of the ^{12}CO $J = 10$–9 (red square symbols) and H_2O 2_{02}-1_{11} (988 GHz; blue crosses) transitions versus the bolometric luminosity of the source, L_{bol}. Strong correlations between L_{bol} and the line luminosity of the ^{12}CO (dotted line) and H_2O (dashed line) transitions are measured.

sample of YSOs composed of 45 low-mass protostars and 86 embedded objects located in the Cygnus X star-forming region. By increasing the sample, the results obtained for WISH can be evaluated over a more statistically supported framework. Similar results as for WISH are achieved when analysing the water line profile of this sample, in particular those regarding the cavity shock component. This work is part of San José-García et al. in preparation.

Future outlook

The *Herschel Space Observatory* unveiled the inner, warmer regions of YSOs environments by observing high rotational transitions of several molecules such as water, a tracer of dynamically active processes. The obtained results, especially from large survey programmes, help to broaden our understanding of the star formation in Galactic and extragalactic scales. However, still many questions are unresolved and the next generation of observational facilities with higher sensitivity (and PhD students) are essential to answer them.

The Atacama Large Millimetre/sub-millimetre Array (ALMA) will reveal the physical and chemical conditions of YSOs at milli-arcsecond resolution, corresponding to a few AU in low-mass and a few tens of AU in high-mass YSOs. Therefore, a better and clearer picture of the gas and temperature distribution within the protostellar system will be obtained. ALMA is already a powerful instrument able to unravel the embedded environments of high-mass YSOs, especially in the hunting and characterisation of possible disks in those objects.

The Stratospheric Observatory for Infrared Astronomy (SOFIA) is able to observe high rotational transitions of molecules as CO with heterodyne spectroscopy. Although with limited sensitivity, these observations play an important role on expanding our knowledge on the inner regions of high-mass YSOs, constraining their excitation temperatures and probing the energetic processes within the outflow, such shocks along the jet and the outflow cavity wall.

Finally, the Mid-Infrared Instrument (MIRI) on board of the *James Webb Space Telescope* (JWST) will be able to trace the hot gas in the inner regions of YSO systems, probing as well the material forming the disks.